

ON THE DETECTION OF NON-TRANSITING HOT JUPITERS IN MULTIPLE-PLANET SYSTEMS

SARAH MILLHOLLAND¹, SONGHU WANG^{1,2}, GREGORY LAUGHLIN¹¹Department of Astronomy and Astrophysics, University of California at Santa Cruz, Santa Cruz, CA 95064 and²School of Astronomy and Space Science and Key Laboratory of Modern Astronomy and Astrophysics in Ministry of Education, Nanjing University, Nanjing 210093, China

Draft version September 21, 2018

ABSTRACT

We outline a photometric method for detecting the presence of a non-transiting short-period giant planet in a planetary system harboring one or more longer period transiting planets. Within a prospective system of the type that we consider, a hot Jupiter on an interior orbit inclined to the line-of-sight signals its presence through approximately sinusoidal full-phase photometric variations in the stellar light curve, correlated with astrometrically induced transit timing variations for exterior transiting planets. Systems containing a hot Jupiter along with a low-mass outer planet or planets on inclined orbits are a predicted hallmark of *in situ* accretion for hot Jupiters, and their presence can thus be used to test planetary formation theories. We outline the prospects for detecting non-transiting hot Jupiters using photometric data from typical *Kepler* objects of interest (KOIs). As a demonstration of the technique, we perform a brief assessment of *Kepler* candidates and identify a potential non-transiting hot Jupiter in the KOI-1858 system. Candidate non-transiting hot Jupiters can be readily confirmed with a small number of Doppler velocity observations, even for stars with $V \gtrsim 14$.

1. INTRODUCTION

Hot Jupiters are both the most readily detectable and the best characterized population of extrasolar planets, yet the dominant mechanism of their formation and evolution remains mysterious.

Within the most commonly accepted theoretical paradigm, hot Jupiters are thought to form at large radial distances before moving inward (see e.g. Wu & Murray 2003; Kley & Nelson 2012; Beaugé & Nesvorný 2012). Several groups have recently proposed theories (Batygin et al. 2015; Boley et al. 2016) that contrast with the established ideas of disk migration and suggest that many hot Jupiters form *in situ* via gas accretion onto 10 - 20 M_{\oplus} cores. Batygin et al. (2015) suggest that, under an *in situ* formation scenario, hot Jupiters should frequently be accompanied by low-mass companions with periods $P \lesssim 100$ d, sometimes with substantial mutual inclinations. Therefore, the presence or absence of close-in companions to hot Jupiters, with or without mutual inclination, provide a potential zeroth-order test for *in situ* formation.

Hot Jupiters are thought to largely lack close coplanar planetary companions. This conclusion stems from a paucity of detections of transiting companions to hot Jupiters in *Kepler* data (Steffen et al. 2012; Latham et al. 2011) and a lack of transit timing variations for these objects (e.g. Gibson et al. 2009). A recent, K2-facilitated discovery (Becker et al. 2015), however, of two close companions to the previously discovered hot Jupiter, WASP 47-b, affirms that hot Jupiters can indeed have close planetary companions. Moreover, in a recent search, Huang et al. (2016) probed all *Kepler* confirmed and candidate transiting hot Jupiters ($P < 10$ d) and warm Jupiters ($10 < P < 200$ d) for transiting companions. While the hot Jupiters have no detectable inner or outer companions with periods $P < 50$ d and radii

$R > 2 R_{\oplus}$, about half of the warm Jupiters are closely accompanied by small planets. The authors point to this as evidence supporting an *in situ* formation scenario for warm Jupiters.

The transit searches used by Steffen et al. (2012) and Huang et al. (2016) place constraints on interior, coplanar companions, but they are less sensitive to exterior planets and are altogether incapable of constraining inclined companions. Furthermore, current radial velocity residuals in systems containing a short-period giant planet are generally at or above the precision required for super-Earth detection. Many low-mass companions to RV-observed hot Jupiters may therefore be lost in the noise.¹

Here, we outline a novel technique for detecting *non-transiting* hot Jupiters in systems containing known transiting planets. Our method synergistically combines two well-known detection and characterization strategies: optical phase curve analysis and transit timing variations (TTVs). Specifically, we aim to simultaneously detect measurements of an optical reflection phase curve due to a non-transiting hot Jupiter in conjunction with reflex motion induced (astrometric) TTVs of an outer, transiting, low-mass planet due to the inclined hot Jupiter. The two measurements must be mutually consistent.

In this paper we detail this “phase+astrometric TTV” method as a technique to search for non-transiting hot Jupiters in systems containing confirmed or candidate planets. In §2, we describe the nature of astrometrically induced TTVs due to a non-transiting hot Jupiter. In §3, we review the usage of optical phase curves for the detection and characterization of giant planets. In §4, we

¹ Adopting a simple mass-radius relationship, $M_p/M_{\oplus} = (R_p/R_{\oplus})^2$, one finds that the median radial velocity half-amplitude for *Kepler* candidate planets is $K = 1.03 \text{ m s}^{-1}$, whereas the median RMS Doppler residual for currently known hot Jupiters (as tabulated at www.exoplanets.org) is $\sigma = 8.9 \text{ m s}^{-1}$

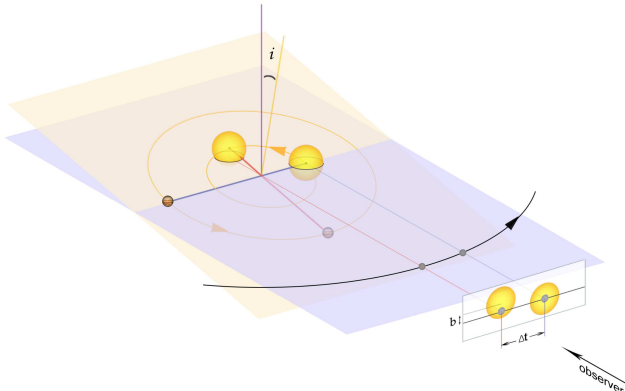


Figure 1. A diagram depicting the physical origin of astrometric TTVs. An orbiting planet, shown in gray and orbiting in the light purple plane, transits at different times due to the reflex motion of the star orbiting a non-transiting HJ in the yellow orbital plane.

analyze the detectability of prospective systems. Finally, in §5 and §6, we describe a brief search of the *Kepler* archived light curves and present a possible candidate non-transiting hot Jupiter in the KOI-1858 system.

2. TRANSIT TIMING VARIATIONS OF AN OUTER PLANET DUE TO AN INTERIOR, NON-TRANSITING HOT JUPITER

If an interior, non-transiting hot Jupiter is present in a system hosting a low-mass transiting planet, the HJ will produce small yet detectable non-uniformities in the transiting object’s inter-transit times. TTVs of this type are astrometrically induced via the HJ’s gravitational effect on the host star and are therefore exceptionally simple to evaluate.

TTVs are most often used to detect planets at or near orbital resonance with a known transiting planet. As such, they depend on planet-planet gravitational effects and often require N-body calculations. In contrast, TTVs of the type analyzed here do not, to first order, depend on planet-planet interactions.

Consider, for example, a planetary system containing a HJ and an outer, transiting, super-Earth (Figure 1). The outer planet’s contribution to the system’s total mass is negligible, so all three bodies may be considered to orbit the star/HJ barycenter. As the HJ orbits, its gravitational influence causes the star to wobble. The outer planet thus orbits a “moving target”, producing astrometric TTVs fully analogous to those found in a circumbinary planetary system (Armstrong et al. 2013).

It is straightforward to derive an approximate model for the theoretically expected TTVs of an outer planet due an inner perturbing HJ. For simplicity, we adopt circular orbits for the HJ and outer planet, and we consider the case where the HJ’s inclination with respect to the orbital plane of the transiting planet is small.

With these assumptions, the TTVs are uniquely specified with only the period of the HJ P_J , the period of the planet P_P , the mass of the star M_* , the mass of the HJ M_J , and the orbital phases ϕ_* and ϕ_P .

The transit times of the outer planet occur when the projected distance between the centers of the star and planet is zero. In terms of the observable quantity $n = 2\pi/P$, this amounts to, assuming $M_* \gg M_J$,

$$\frac{1}{(n_J)^{\frac{2}{3}}} \frac{M_J}{M_*} \cos(n_J t + \phi_*) - \frac{1}{(n_P)^{\frac{2}{3}}} \cos(n_P t + \phi_P) = 0. \quad (1)$$

The outer planet’s mid-transit times are times, t , approximately periodic in P_P , that satisfy this expression. The maximum amplitude of the variations in the inter-transit times is given by

$$\Delta T_{\text{TTV}} = \frac{1}{\pi} P_P^{1/3} P_J^{2/3} \frac{M_J}{M_*}. \quad (2)$$

In addition to the timing variations, a non-transiting HJ also induces transit *duration* variations (TDVs) for planet P. With the assumptions that lead to Equation 2, the transit durations differ by up to

$$\Delta T_{\text{TDV}} = \frac{4R_*}{(2\pi GM_*)^{1/3}} \frac{M_J}{M_*} \left(\frac{P_P^2}{P_J} \right)^{1/3} \quad (3)$$

depending on whether the HJ is at inferior or superior conjunction when the transits occur.

For the fiducial case of $M_{\text{HJ}} = M_{\text{Jup}}$, $P_{\text{HJ}} = 3$ d, $P_P = 50$ d, $M_* = M_\odot$, and $R_* = R_\odot$, this results in a TTV amplitude of $\Delta T_{\text{TTV}} = 3.4$ min and a TDV amplitude of $\Delta T_{\text{TDV}} = 2.0$ min. These signals are both detectable given a light curve with small enough photometric precision.

If there is a large mutual inclination between the HJ’s and outer planet’s orbital planes, the TDVs can be larger, due to variation in the impact parameter of the transit chord (see Figure 1). In this case there is a trade-off between the TTV and TDV amplitudes, depending on the observer’s viewing orientation. For photometry of sufficient quality, the timing and geometric constraints enable a *complete* description of the HJ’s orbit.

3. OPTICAL PHASE CURVES

In the absence of an independent estimate of the HJ’s orbital period, the prospects for detecting non-transiting HJs using *Kepler*-quality TTVs and TDVs appear bleak. Fortunately, the detection of an optical reflected light phase curve can combine with the TTVs to yield a highly constrained problem.

Out-of-transit, optical phase-folded light curves are already highly effective tools for characterization of giant (stellar or sub-stellar) transiting companions (e.g. Shporer et al. 2011; Shporer & Hu 2015; Esteves et al. 2013, 2015). The phase curve, composed of photometry across the out-of-transit orbit, results from the superposition of several independent effects: reflected light and thermal emission, Doppler boosting (beaming) from the reflex motion of the star, and ellipsoidal variations due to tidal forces exerted on the star by the companion (Shporer et al. 2011). The BEER model (Faigler & Mazeh 2011) has become an effective tool for simultaneously analyzing these three components.

For the typical HJ ($P \sim 3$ d, $M \sim 1 M_{\text{Jup}}$), reflection is the strongest component, over one order of magnitude greater than the beaming and ellipsoidal components. The phase curve in these circumstances is, to first order, sinusoidal.

While several groups have performed a comprehensive search for phase curve variations in *transiting* HJs (e.g. Esteves et al. 2015), none have undertaken a thorough

search for phase curve detections of *non-transiting* HJs, although authors have frequently discussed the prospects of discovering non-transiting massive planets via their phase curves (e.g. Shporer & Hu 2015). Moreover, phase curves have been used to discover small, non-eclipsing binary stars ($0.07 - 0.4 M_{\odot}$), in which cases all three phase curve components have significant amplitudes (Faigler et al. 2012). With the reflection-dominated phase curves of HJs, however, the signals are much more prone to false positives. Fortunately, the simultaneous detection of a reflection-dominated phase curve with astrometric TTVs breaks this degeneracy.

4. DETECTABILITY: ANALYSIS OF A FIDUCIAL SYSTEM

We now consider the detectability of a non-transiting, typical HJ in a fiducial system containing an outer, transiting, low-mass planet. We show that the unseen giant planet is readily detectable given *Kepler*-quality photometry.

Consider a hypothetical planetary system: a $1 M_{\odot}$, $1 R_{\odot}$ host star; a $1 M_{\text{Jup}}$, $1.3 R_{\text{Jup}}$ HJ on a $P_{\text{J}} = 3$ d orbit with geometric albedo $A_{\text{g}} = 0.2$; and a $2 R_{\oplus}$ planet on a $P_{\text{P}} = 20.6$ d orbit. Assume the HJ's orbit is slightly inclined to the line of sight ($i \sim 85^{\circ}$), yielding a 45 ppm phase curve amplitude. (Note that even with $i \sim 45^{\circ}$, the amplitude is still ~ 30 ppm, similar to *Kepler*'s median combined differential photometric precision of 29 ppm for 6.5 hr integrations of $V = 12$ mag stars.)

We inserted the HJ's sinusoidal phase curve into a 330 day, 30 minute cadence light curve with 150 ppm precision. This corresponds to approximately 4 quarters of *Kepler* long cadence photometry on a typical $V \sim 13$ mag star.

In a Lomb-Scargle (LS) periodogram (Lomb 1976; Scargle 1982) of the light curve, over a 1-5 day range, the 3 d signal is easily the highest peak. A Gaussian fit to the highest peak in the periodogram yields $P_{\text{J}} = 3.002 \pm 0.01$. A least-squares sine fit to the phase-folded light curve, binned such that 400 points span the orbit, returns an amplitude of ~ 43 ppm, close to the 45 ppm input. The recovered phase curve is shown in Figure 2.

The astrometric TTVs of the $2 R_{\oplus}$ planet form a roughly sinusoidal oscillation with amplitude ~ 1.25 min and period ~ 150 d. This is not easy to detect given the 2-4 minute uncertainties that are typical for *Kepler* TTVs of a $2 R_{\oplus}$ planet orbiting a $V \sim 13$, $1 R_{\odot}$ star.

Figure 2 shows the expected TTVs with scatter consistent with typical observational uncertainty. When comparing the TTV model with data, it is important to note that the TTV phase may be uniquely determined using the epoch of the phase curve maximum. Although a visual comparison between the TTV model and simulated data is suggestive at best, the LS periodograms of the model and data show a strong correspondence (Figure 3). Each periodogram has a easily detectable peak near ~ 155 d.

The phase curve and astrometric TTVs of this fiducial system are both readily detectable given *Kepler*-quality photometry. Although neither signal would itself yield a conclusive detection, the combination of the two, coupled with the demand of phase correlation, is extremely powerful. Promising candidates, furthermore, can readily be confirmed using RV measurements.

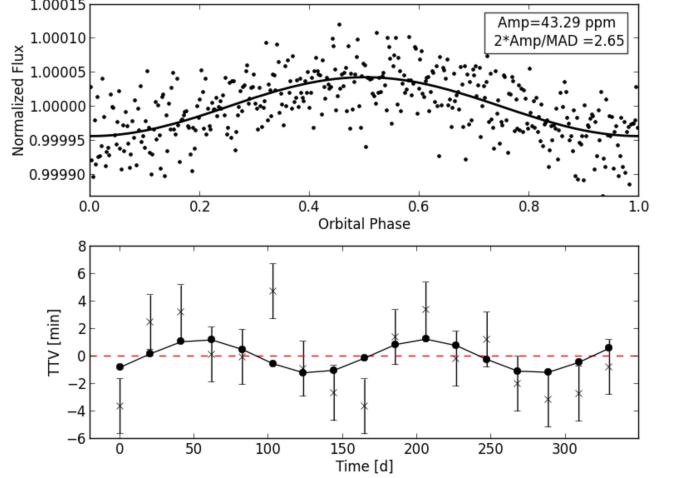


Figure 2. The detected phase curve and TTVs for a fiducial system. The phase curve is folded with period $P = 3.002$ d and binned such that 400 points span the orbit. The black line indicates a sinusoidal fit. In the TTV plot, the “x” symbols represent the synthetic data consistent with typical observational uncertainty, and the black dots are the underlying model.

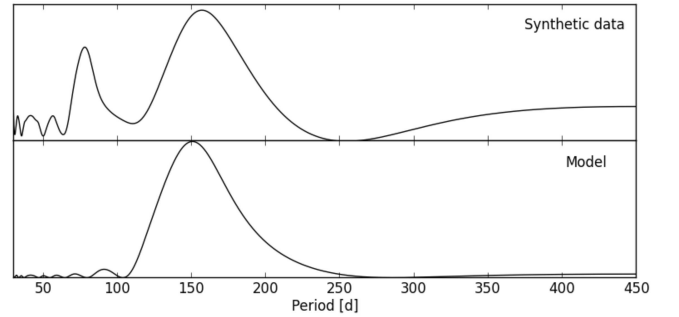


Figure 3. The LS periodograms of the TTVs for the synthetic data (top) and model TTVs (bottom). Each features a ~ 155 d peak, which would become sharper given a longer baseline of data.

5. CANDIDATE NON-TRANSITING HOT JUPITERS IN THE *KEPLER* DATA

We performed a brief assessment of the archived *Kepler* data to search for non-transiting HJs using the “phase+astrometric TTV” technique. Our analysis has been in no way comprehensive, so we suggest a future thorough search.

We examined a subset of targets flagged as confirmed exoplanets or KOIs from the MAST *Kepler* data archive². We used the publicly available light curve files containing the pre-search data conditioning (PDC) simple aperture photometry (Stumpe et al. 2012). We only considered data from *Kepler* operational quarters 13 through 17, to decrease initial computational costs. We used publicly available TTV data calculated using long cadence data from *Kepler* quarters 1 through 12 (Mazeh et al. 2013).

We first searched the light curves for phase curve detections. We filtered the light curves by removing variability on timescales greater than 6 d using the *kepflatten* routine in the *PyKE Kepler* data reduction software (Still & Barclay 2012). We then removed 2σ outliers and stitched

² <https://archive.stsci.edu/Kepler/>

the light curves from various quarters and cadence modes together.

Operating on these detrended and concatenated light curves, we calculated each target's Lomb-Scargle (LS) periodogram in a 1 to 5 day period range. We folded the light curve according to the peak period in the periodogram and performed a least-squares sinusoidal fit to the resulting phase curve. The best-fit amplitude provides a criterion for false positives, as the signals of HJ phase curves have only been observed up to ~ 70 ppm (Esteves et al. 2015). The phase of the fit is used to derive a time epoch at which the HJ is directly behind the star, to within uncertainties caused by possible shifts between the brightest region on the planet and the substellar point (as discussed in Shporer & Hu 2015).

At this stage, many of the target light curves show roughly sinusoidal phase curve variations. Several are likely false positives due to contamination from stellar variability. The TTVs help rule out these false positives, but autocorrelations could be another effective technique. While stellar variability changes in phase, period, and amplitude as time progresses, an orbital phase curve remains strictly uniform.

For each *Kepler* confirmed planet/KOI in our selection, we generated a profile of the expected TTVs to compare them to the Mazeh et al. (2013) observed TTVs. In the TTV calculations, we used the period of the HJ as detected from the phase curve, the average period of the planet/KOI as detected from its transits and reported at the NASA Exoplanet Archive³, the stellar mass estimated from stellar parameters and the planetary transit model fitting, a fiducial HJ mass of $1 M_{\text{Jup}}$, and ϕ_{P} and ϕ_{\star} derived from the time epochs of the transit and the phase curve maximum.

We compared each candidate's modeled and observed TTVs and simultaneously visually examined the candidates' detected phase curves. We also visually compared the LS periodograms of the expected and observed TTVs. We established a list of ~ 20 candidates showing both detectable phase curve variations and TTVs for which the data and model qualitatively matched within observational uncertainty.

6. A CANDIDATE NON-TRANSITING HOT JUPITER IN THE KOI-1858 SYSTEM

Here we present one of our detected candidates, a possible non-transiting HJ orbiting *Kepler* star 8160953. This star has $T_{\text{eff}} \sim 5400K$ (Everett et al. 2013), mass $0.981^{+0.131}_{-0.097} M_{\odot}$ and radius $0.997^{+0.388}_{-0.111} R_{\odot}$. It hosts KOI-1858.01, a $3.53^{+1.38}_{-0.39} R_{\oplus}$ candidate planet in a 116.3319 ± 0.0014 d orbit, and KOI-1858.02, a $2.06^{+0.8}_{-0.23} R_{\oplus}$ candidate planet in a 86.049 ± 0.007 d orbit³.

Using all available light curve data, the LS periodogram returns a strong, ~ 52 ppm amplitude phase curve detection with period 2.993 ± 0.018 d. The phase curve and a sinusoidal fit are shown in Figure 4.

Moreover, the theoretically expected TTVs of KOI-1858.01 are consistent with the Mazeh et al. (2013) TTV data within observational uncertainty. Unfortunately, the uncertainties of the TTV measurements for KOI-1858.02 are too large for a suitable comparison. To rigor-

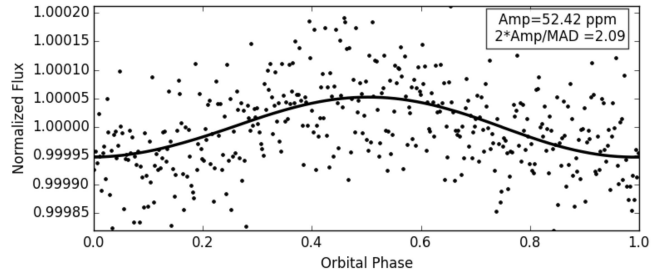


Figure 4. The detected phase curve for the candidate non-transiting HJ in the KOI-1858 system. The light curve was phase-folded at the post-MCMC period estimate, 2.991 d, and binned such that 400 points span the orbit. The black line is a fixed-period, least-squares sinusoidal fit, returning a ~ 52 ppm amplitude estimate.

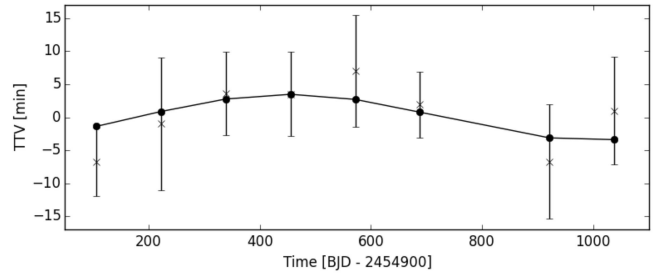


Figure 5. The MCMC derived fit to KOI-1858.01's observed TTVs. The "x" symbols represent the data, and the black line is the fit using the parameters of the posterior means.

ously evaluate the consistency between KOI-1858.01's expected and observed TTVs, we performed parameter estimation using the Markov Chain Monte Carlo (MCMC) Metropolis-Hastings algorithm.

The MCMC contained 6 free parameters: M_{\star} , M_{J} , P_{J} , P_{P} , the transit epoch t_0 , and the epoch of the HJ's superior conjunction t_{J} . (ϕ_{P} and ϕ_{\star} in Eqn. 1 are derived from the two time epochs.) Most of these parameters have very tight priors. We used Gaussian priors with means and standard deviations for M_{\star} , P_{P} , and t_0 derived from the transit model fit as reported on the NASA Exoplanet Archive³. The prior distribution for P_{J} was derived from a Gaussian fit to the peak period in the LS periodogram. The prior mean for t_{J} was estimated from the sinusoidal fit to the phase curve, and the standard deviation was taken to be 0.3 d, which is 10% of the orbit. The prior mean and standard deviation for M_{J} were $1.5 M_{\text{Jup}}$ and $0.5 M_{\text{Jup}}$, respectively.

The likelihood of the TTV data \mathbf{d} given the set $\boldsymbol{\theta}$ of model parameters is given by $L(\mathbf{d}|\boldsymbol{\theta}) \propto e^{-\alpha\chi^2}$ where χ^2 is the usual definition of the chi-square error and α is a scaling parameter.

We used the Metropolis-Hastings algorithm to sample from the posterior distribution given these priors and likelihood. We removed one outlier from the TTV data corresponding to a section of missing data in the light curve. The TTV model fit using the best-fit parameters (posterior means) after 1000000 samples is presented in Figure 5. The posterior means of M_{\star} , P_{P} , and t_0 are consistent with the prior means, as they should be. The best-fit estimates for the HJ's parameters are as follows: $P_{\text{J}} = 2.991 \pm 0.0019$ d, $M_{\text{J}} = 1.5 \pm 0.4 M_{\text{Jup}}$, and $t_{\text{J}} = 2454966.82 \pm 0.24$ BJD. Using the mass/radius

³ <http://exoplanetarchive.ipac.caltech.edu>

distribution of known HJs with $P < 5$ d, the HJ mass estimate is consistent with a radius of $1.34 \pm 0.74 R_{\text{Jup}}$. For consistency with the ~ 52 ppm phase curve amplitude, the HJ's geometric albedo should be ~ 0.2 , which is a physically reasonable estimate. Moreover, the best-fit estimate for t_{J} is consistent with the epoch of the phase curve maximum, 2454966.77 BJD, meaning the two independent measurements are phase correlated.

Although TDVs were detected for KOI-1858.01 by [Mazeh et al. \(2013\)](#), the observational uncertainties were too large for a rigorous examination here. It should be noted, however, that the observed TDVs are not in disagreement with the expected signal due to a non-transiting HJ. We suggest a future detailed analysis of KOI-1858.01's TTVs and TDVs using all 17 quarters of *Kepler* data. This further information may enable a full description of the candidate HJ's orbit.

Despite *Kepler* 8160953 being fairly dim ($V \sim 14.7$), the non-transiting HJ candidate is readily RV-confirmed given its large expected Doppler half-amplitude, $K \sim 214$ m/s. This is easily detectable on a telescope like the Automated Planet Finder, which will attain 30-40 m/s precision in a 1 hr measurement. Moreover, the epoch of superior conjunction t_{J} and orbital period P_{J} estimates can be used to precisely specify the quadrature ephemeris.

7. CONCLUSION

We have shown that the combination of full phase light curves and astrometric transit timing variations generates an effective method for identifying non-transiting HJs in multiple-planet systems, and as a proof of concept, we identified a candidate non-transiting HJ in the *Kepler* 8160953/KOI-1858 system. If we assume that $\sim 3,000$ stars among the $\sim 150,000$ monitored by *Kepler* will be confirmed to harbor transiting super-Earths, and if we assume that *in situ* formation is a significant channel for creating HJs (which have an intrinsic occurrence fraction of $\sim 0.5\%$), then we expect that ~ 10 non-transiting HJs can be identified using the method outlined here and confirmed using quick-look Doppler spectroscopy. It also bears mentioning that photometric data from the K2 and TESS Missions will be equally

well suited to identifying such systems.

We acknowledge support from the NASA Astrobiology Institute through a cooperative agreement between NASA Ames Research Center and the University of California at Santa Cruz, and from the NASA TESS Mission through a cooperative agreement between M.I.T. and UCSC.

REFERENCES

- Armstrong, D., Martin, D. V., Brown, G., et al. 2013, MNRAS, 434, 3047
- Batygin, K., Bodenheimer, P. H., & Laughlin, G. P. 2015, ArXiv e-prints, arXiv:1511.09157
- Beaugé, C., & Nesvorný, D. 2012, ApJ, 751, 119
- Becker, J. C., Vanderburg, A., Adams, F. C., Rappaport, S. A., & Schwengeler, H. M. 2015, ApJ, 812, L18
- Boley, A. C., Granados Contreras, A. P., & Gladman, B. 2016, ApJ, 817, L17
- Esteves, L. J., De Mooij, E. J. W., & Jayawardhana, R. 2013, ApJ, 772, 51
- . 2015, ApJ, 804, 150
- Everett, M. E., Howell, S. B., Silva, D. R., & Szkody, P. 2013, ApJ, 771, 107
- Faigler, S., & Mazeh, T. 2011, MNRAS, 415, 3921
- Faigler, S., Mazeh, T., Quinn, S. N., Latham, D. W., & Tal-Or, L. 2012, ApJ, 746, 185
- Gibson, N. P., Pollacco, D., Simpson, E. K., et al. 2009, ApJ, 700, 1078
- Huang, C. X., Wu, Y., & Triaud, A. H. M. J. 2016, ArXiv e-prints, arXiv:1601.05095
- Kley, W., & Nelson, R. P. 2012, ARA&A, 50, 211
- Latham, D. W., Rowe, J. F., Quinn, S. N., et al. 2011, ApJ, 732, L24
- Lomb, N. R. 1976, Ap&SS, 39, 447
- Mazeh, T., Nachmani, G., Holczer, T., et al. 2013, ApJS, 208, 16
- Scargle, J. D. 1982, ApJ, 263, 835
- Shporer, A., & Hu, R. 2015, AJ, 150, 112
- Shporer, A., Jenkins, J. M., Rowe, J. F., et al. 2011, AJ, 142, 195
- Steffen, J. H., Ragozzine, D., Fabrycky, D. C., et al. 2012, Proceedings of the National Academy of Science, 109, 7982
- Still, M., & Barclay, T. 2012, PyKE: Reduction and analysis of Kepler Simple Aperture Photometry data, Astrophysics Source Code Library, ascl:1208.004
- Stumpe, M. C., Smith, J. C., Van Cleve, J. E., et al. 2012, PASP, 124, 985
- Wu, Y., & Murray, N. 2003, ApJ, 589, 605